

Ferromagnetic planar Josephson junction with transparent interfaces: a ϕ junction proposal

This article has been downloaded from IOPscience. Please scroll down to see the full text article.

2013 J. Phys.: Condens. Matter 25 215701

(<http://iopscience.iop.org/0953-8984/25/21/215701>)

View [the table of contents for this issue](#), or go to the [journal homepage](#) for more

Download details:

IP Address: 213.131.11.41

The article was downloaded on 05/06/2013 at 07:47

Please note that [terms and conditions apply](#).

Erratum: Ferromagnetic planar Josephson junction with transparent interfaces: a φ junction proposal

2013 *J. Phys.: Condens. Matter* **25** 215701

D M Heim¹, N G Pugach^{2,3}, M Yu Kupriyanov², E Goldobin⁴, D Koelle⁴ and R Kleiner⁴

¹ Institut für Quantenphysik and Center for Integrated Quantum Science and Technology (IQST), Universität Ulm, D-89069 Ulm, Germany

² Skobeltsyn Institute of Nuclear Physics, M V Lomonosov Moscow State University, 119991 Leninskie Gory, Moscow, Russia

³ Faculty of Physics, M V Lomonosov Moscow State University, 119991 Leninskie Gory, Moscow, Russia

⁴ Physikalisches Institut and Center for Collective Quantum Phenomena in LISA⁺, Universität Tübingen, D-72076 Tübingen, Germany

E-mail: dennis.heim@uni-ulm.de

Received 9 May 2013

Published 17 May 2013

Online at stacks.iop.org/JPhysCM/25/239601

The following corrections must be made due to errors that occurred during the production of this paper.

- On page 1 the references in the sentence ‘Since then φ junctions have been studied more and more intensively...’ should be [2, 3, 9–14].
- On page 1 the references in the sentence ‘Only recently, experimental evidence of a φ junction...’ should be [2, 11, 12].
- On page 1 the references in the sentence ‘On the other hand this φ junction concept...’ should be [11, 12, 15].
- Equation (23) should read

$$I_{F,\text{dir}}(\phi) = 64\sqrt{2}d_{F\kappa} e^{-2\kappa L} \mathcal{F} \sin\left(2\kappa L + \frac{\pi}{4}\right) \sin\phi. \quad (23)$$

- References [4], [25] and [27] should be written in the form
[4] Bulaevskii L N, Kuzii V V and Sobyenin A A 1977 *Pis'ma Zh. Eksp. Teor. Phys.* **25** 314–318
Bulaevskii L N, Kuzii V V and Sobyenin A A 1977 *JETP Lett.* **25** 290–294 (Engl. transl.)
[25] Buzdin A I and Kupriyanov M Yu 1991 *Pis'ma Zh. Eksp. Teor. Phys.* **53** 308–312
Buzdin A I and Kupriyanov M Yu 1991 *JETP Lett.* **53** 321–326 (Engl. transl.)
[27] Kupriyanov M Yu and Lukichev V F 1988 *Zh. Eksp. Teor. Fiz.* **94** 139–149
Kupriyanov M Yu and Lukichev V F 1988 *Sov. Phys. JETP* **67** 1163–1168 (Engl. transl.)

Ferromagnetic planar Josephson junction with transparent interfaces: a φ junction proposal

D M Heim¹, N G Pugach^{2,3}, M Yu Kupriyanov², E Goldobin⁴, D Koelle⁴
and R Kleiner⁴

¹ Institut für Quantenphysik and Center for Integrated Quantum Science and Technology (IQST),
Universität Ulm, D-89069 Ulm, Germany

² Skobeltsyn Institute of Nuclear Physics, M V Lomonosov Moscow State University, 119991 Leninskie
Gory, Moscow, Russia

³ Faculty of Physics, M V Lomonosov Moscow State University, 119991 Leninskie Gory, Moscow,
Russia

⁴ Physikalisches Institut and Center for Collective Quantum Phenomena in LISA⁺, Universität
Tübingen, D-72076 Tübingen, Germany

E-mail: dennis.heim@uni-ulm.de

Received 18 February 2013, in final form 20 March 2013

Published 2 May 2013

Online at stacks.iop.org/JPhysCM/25/215701

Abstract

We calculate the current-phase relation of a planar Josephson junction with a ferromagnetic weak link located on top of a thin normal metal film. Following experimental observations we assume transparent superconductor–ferromagnet interfaces. This provides the best interlayer coupling and a low suppression of the superconducting correlations penetrating from the superconducting electrodes into the ferromagnetic layer. We show that this Josephson junction is a promising candidate for experimental φ junction realization.

(Some figures may appear in colour only in the online journal)

1. Introduction

A φ junction [1, 2] is a Josephson junction with a doubly degenerate ground state, in which the Josephson phase takes the values $+\varphi$ or $-\varphi$ ($0 < \varphi < \pi$) [3]. This junction being closed into a ring is able to self-generate a fractional flux $\Phi_0\varphi/(2\pi)$, where Φ_0 is the magnetic flux quantum.

In this sense the φ junction is a generalization of the π junction [4] which has a Josephson phase $+\pi$ or $-\pi$ in its ground state. It has been experimentally demonstrated that the π junction improves the performance and simplifies the design of classical and quantum circuits [5–7]. Since the φ junction offers the possibility to choose a special value for the phase in the ground state it may further optimize these circuits.

The initial φ junction proposal [1] dealt with grain boundary junctions, where the critical current density $j_c(x)$ quickly oscillates along the Josephson junction barrier. A similar system, where $j_c(x)$ is a random function of x , was studied experimentally [8]. A positive as well as a negative

second harmonic in the current-phase relation (CPR) for different samples were detected. However, no clear evidence of φ junction behaviour was demonstrated.

Since then φ junctions have been studied more and more intensively and many other systems have been proposed as possible candidates for the realization of φ junctions e.g. [2, 3, 9–12, 14]. Only recently, experimental evidence of a φ junction made of 0 and π parts [2, 11, 13] was reported [15]. One half of the junction had the Josephson phase 0 in its ground state and the other half the phase π . This was realized [15] by connecting two superconductor–insulator–ferromagnet–superconductor (SIFS) junctions in parallel. The advantage of this concept is that it is based on the technology already developed for the fabrication of 0– π junctions [16, 17].

On the other hand this φ junction concept is difficult to realize experimentally because, e.g., a step in the thickness of the F layer must be realized with very high accuracy [11, 13, 15]. A different method, the ‘ramp-type overlap’ (RTO) φ

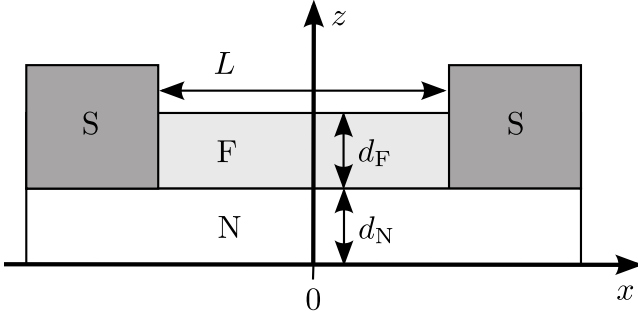


Figure 1. The geometry of the considered system. The Josephson junction consists of two superconducting (S) electrodes separated by a ferromagnetic (F) weak link of thickness d_F and length L . It is located on top of a thin normal (N) metal film of thickness d_N .

junction, was proposed by Bakurskiy *et al* [18]. This method only requires one small SFS junction located on a thin normal (N) metal layer, see figure 1. This basic setup provides a miniaturized φ junction. Moreover, this type of junction has already been realized experimentally for the analysis of the double proximity effect [19].

A simple model [3] to show that the RTO junction can be used as a φ junction requires its CPR. By writing it in terms of a sine series

$$I(\phi) = A \sin(\phi) + B \sin(2\phi), \quad (1)$$

where ϕ is the Josephson phase, the amplitudes have to obey the conditions [3]

$$|B| > |A|/2 \quad \text{and} \quad B < 0. \quad (2)$$

The RTO junction, schematically shown in figure 1, can fulfil these conditions because the current flows between the S electrodes through the F metal and the N layer. In this way the properties of an SFS and SNS junction are combined. The SFS junction can have a negative [20, 21] amplitude A_F in (1), while the SNS junction has a positive [20, 22] amplitude A_N in (1). By adding both, the total amplitude A can be minimized and a dominant negative amplitude B from the SNS part is obtained to fulfil conditions (2). Since supercurrents in SFS junctions are rather small, the SNS contribution has to be reduced. This is done by using only a thin normal metal film.

In this paper we investigate an RTO junction which has, differently from the one proposed in [18], transparent SF interfaces in order to amplify the SFS contribution to the total current. This assumption has already successfully been used to describe various experiments [19, 23, 24]. As a result, we obtain slightly smaller system sizes for the φ junction realization than [18], where weakly transparent interfaces were assumed. Moreover, our approach provides a better penetration of the superconducting correlations into the F layer which may increase the Josephson current. In the framework of transparent SF interfaces we cannot use linearized equations for the SFS part, as was done in [18]. Therefore, we use non-linearized equations in the SFS and SNS part for our analytical approach.

We derive the CPR in the ‘dirty’ limit. For this purpose, we combine the solution for the Usadel equations in the N

film [18] with the solution for the Usadel equations in the SFS layer [25]. The resulting current-phase relation consists of three parts: (i) a contribution from the SFS layer, (ii) a contribution from the N film and (iii) a composite SNFS term.

The paper is organized as follows. In section 2 we introduce the model of the considered Josephson junction in terms of Usadel equations. The analytical expression for the CPR of our system is based on this model and presented in section 3. In section 4 we use this expression together with realistic system parameters to discuss its applicability as a φ junction. Finally, an appendix provides a detailed derivation of the composite SNFS current.

2. Model

The considered Josephson junction is sketched in figure 1. It consists of an SFS junction located on a normal metal film. The F layer has a thickness d_F and a length L while the N layer has a thickness d_N and is considered as infinitely long. We have chosen the x and z axis in directions parallel and perpendicular to the plane of the N film, respectively.

For the calculation of the current $I(\phi)$ flowing from one superconducting electrode to the other we determine the Green’s functions describing our system. Since experiments similar to our proposal are performed in the ‘dirty’ limit [19, 23, 24], in which the elastic scattering length is much smaller than the characteristic decay length, we can use the Usadel equations [26] to model our system. We write them in the form [20]

$$\xi_j^2 \left[\frac{\partial}{\partial x} \left(G_j^2 \frac{\partial}{\partial x} \Phi_j \right) + \frac{\partial}{\partial z} \left(G_j^2 \frac{\partial}{\partial z} \Phi_j \right) \right] - \frac{\tilde{\omega}}{\pi T_c} \Phi_j = 0, \quad (3)$$

$$G_j = \frac{\tilde{\omega}}{\sqrt{\tilde{\omega}^2 + \Phi_j \Phi_j^*}}, \quad j \in \{N, F\}$$

in the N and F layer, respectively. Here, Φ_j and G_j are the Usadel Green’s functions in the Φ parametrization [27]. The frequencies $\tilde{\omega} = \omega + iH$ contain the Matsubara frequencies $\omega = \pi T(2n + 1)$ at temperature T , where $n = 0, 1, 2, \dots$, and the exchange field H of the ferromagnetic material which is assumed to be zero in the N layer. The decay lengths

$$\xi_N = \sqrt{\frac{D_N}{2\pi T_c}}, \quad \xi_F = \sqrt{\frac{D_F}{2\pi T_c}} \quad (4)$$

of the superconducting correlations are defined via the critical temperature T_c of the superconductor (we use $\hbar = k_B = 1$) and the diffusion coefficients D_N and D_F in the normal and ferromagnetic metal, respectively.

We assume that superconductivity in the S electrodes is not suppressed by the neighbouring N and F layers. This assumption is valid in our case of transparent SF interfaces with the conditions for the suppression parameters

$$\gamma_{BSF} = \frac{R_{BSF} A_{BSF}}{\rho_F \xi_F} \ll 1, \quad \gamma_{SF} = \frac{\rho_S \xi_S}{\rho_F \xi_F} \ll 1, \quad (5)$$

$$\gamma_{BSN} = \frac{R_{BSN} A_{BSN}}{\rho_N \xi_N} \gg \gamma_{SN} = \frac{\rho_S \xi_S}{\rho_N \xi_N}. \quad (6)$$

Here, $R_{\text{BSN,BSF}}$ and $A_{\text{BSN,BSF}}$ are the resistances and areas of the SN and SF interfaces. The values for $\rho_{\text{N,F,S}}$ describe the resistivity of the N, F, and S metals, respectively.

This allows us to use the rigid boundary conditions [20]

$$\Phi_{\text{S}}(\pm L/2) = \Delta \exp(\pm i\phi/2), \quad G_{\text{S}} = \frac{\omega}{\sqrt{\omega^2 + \Delta^2}}, \quad (7)$$

where Δ is the absolute value of the order parameter in the superconductor.

The boundary conditions [27, 28, 20] at the free interfaces are

$$\frac{\partial}{\partial z} \Phi_j = 0, \quad j \in \{\text{N, F}\}, \quad (8)$$

and at the interfaces of the superconductor they are

$$\gamma_{\text{BSN}} \xi_{\text{N}} \frac{\partial \Phi_{\text{N}}}{\partial z} = \frac{G_{\text{S}}}{G_{\text{N}}} [\Phi_{\text{S}}(\pm L/2) - \Phi_{\text{N}}] \quad (9)$$

and

$$\Phi_{\text{F}} = \frac{\tilde{\omega}}{\omega} \Phi_{\text{S}}(\pm L/2). \quad (10)$$

Additionally we use

$$\gamma_{\text{BNF}} \xi_{\text{F}} \frac{\partial \Phi_{\text{F}}}{\partial z} = \frac{G_{\text{N}}}{G_{\text{F}}} \left(\frac{\tilde{\omega}}{\omega} \Phi_{\text{N}} - \Phi_{\text{F}} \right) \quad (11)$$

at the NF interfaces, where

$$\gamma_{\text{BNF}} = \frac{R_{\text{BNF}} A_{\text{BNF}}}{\rho_{\text{F}} \xi_{\text{F}}} \quad (12)$$

is defined analogous to (6).

Finally we calculate the total current

$$I(\phi) = I_{\text{N}}(\phi) + I_{\text{F}}(\phi) \quad (13)$$

by integrating the standard expressions [20] for the current densities of the N and F part over the junction cross section along the z axis. This leads us to

$$\begin{aligned} I_{\text{N}}(\phi) = & i \frac{\pi T W}{2e \rho_{\text{N}}} \sum_{\omega=-\infty}^{\infty} \int_0^{d_{\text{N}}} dz \frac{G_{\text{N}}^2}{\omega^2} \\ & \times \left[\Phi_{\text{N}}(\omega) \frac{\partial}{\partial x} \Phi_{\text{N}}^*(-\omega) \right. \\ & \left. - \Phi_{\text{N}}^*(-\omega) \frac{\partial}{\partial x} \Phi_{\text{N}}(\omega) \right]_{x=0} \end{aligned} \quad (14)$$

and

$$\begin{aligned} I_{\text{F}}(\phi) = & i \frac{\pi T W}{2e \rho_{\text{F}}} \sum_{\omega=-\infty}^{\infty} \int_{d_{\text{N}}}^{d_{\text{N}}+d_{\text{F}}} dz \frac{G_{\text{F}}^2}{\tilde{\omega}^2} \\ & \times \left[\Phi_{\text{F}}(\omega) \frac{\partial}{\partial x} \Phi_{\text{F}}^*(-\omega) \right. \\ & \left. - \Phi_{\text{F}}^*(-\omega) \frac{\partial}{\partial x} \Phi_{\text{F}}(\omega) \right]_{x=0}. \end{aligned} \quad (15)$$

The width W of the junction along the y axis is supposed to be small compared to the Josephson penetration depth. We have chosen the position $x = 0$ for integration over the junction cross section since the z component of the current densities

vanishes there due to the symmetry of the considered junction geometry.

3. Currents

In order to calculate the current $I(\phi)$ from (13) we cannot simply add the current through the N layer calculated by Bakurskiy *et al* [18] to the SFS current calculated by Buzdin and Kupriyanov [25] because we have to take into account a composite SNFS current which appears due to a penetration of superconductivity from the N layer into the F layer. Therefore, we split the current $I_{\text{F}}(\phi)$ into a contribution $I_{\text{F,dir}}(\phi)$ due to a direct penetration of superconductivity into the F layer and an additional part $I_{\text{NF}}(\phi)$. This leads us to

$$I(\phi) = I_{\text{N}}(\phi) + I_{\text{F,dir}}(\phi) + I_{\text{NF}}(\phi). \quad (16)$$

In the following three sections we derive the expressions for these three currents using the scaling

$$\tilde{I}_j(\phi) = I(\phi) \frac{e \rho_j}{W \Delta}. \quad (17)$$

3.1. Current in the N layer

In this layer we adopt the current

$$\tilde{I}_{\text{N}}(\phi) = 2 \frac{d_{\text{N}} T}{\xi_{\text{N}} T_{\text{c}}} \sum_{\omega>0} \frac{\Gamma(\phi)}{\mu(\phi)} r \sin(\phi) \quad (18)$$

with the definitions

$$\Gamma(\phi) = \frac{r \delta \sqrt{\gamma_{\text{BM}} \Omega + G_{\text{S}}}}{\sqrt{2 \gamma_{\text{BM}} \Omega (\sqrt{\Omega^2 + \delta^2 r^2} + \mu(\phi))}}, \quad (19)$$

$$\delta = \frac{\Delta}{\pi T_{\text{c}}}, \quad \gamma_{\text{BM}} = \frac{\gamma_{\text{BSN}} d_{\text{N}}}{\xi_{\text{N}}}, \quad \Omega = \frac{\omega}{\pi T_{\text{c}}}, \quad (20)$$

$$r = \left(\frac{\gamma_{\text{BM}}}{\pi T_{\text{c}}} \sqrt{\omega^2 + \Delta^2} + 1 \right)^{-1}, \quad (21)$$

$$\mu(\phi) = \sqrt{\Omega^2 + r^2 \delta^2 \cos^2(\phi/2)} \quad (22)$$

from [18]. Its derivation is based on the assumption $L \ll \xi_{\text{N}}$ and an infinitely long N layer. It is calculated with the help of the solution $\Phi_{\text{N}}(x)$ (A.9) for the non-linear Usadel equations, which depends only on the coordinate x because the thickness $d_{\text{N}} \ll \xi_{\text{N}}$ is assumed to be small.

3.2. Current in the F layer

The current

$$I_{\text{F,dir}}(\phi) = \sqrt{2} d_{\text{F}} \kappa e^{-2\kappa L} \mathcal{F} \sin\left(2\kappa L + \frac{\pi}{4}\right) \sin \phi, \quad (23)$$

with

$$\kappa = \frac{\sqrt{\hbar}}{\sqrt{2} \xi_{\text{F}}}, \quad h = \frac{H}{\pi T_{\text{c}}}, \quad \mathcal{F} = \pi T \sum_{\omega>0} \frac{\Theta^2}{\Delta}, \quad (24)$$

$$\Theta = \frac{\Delta}{\eta + |\omega| + \sqrt{2\eta(\eta + |\omega|)}}, \quad \eta = \sqrt{\omega^2 + \Delta^2}, \quad (25)$$

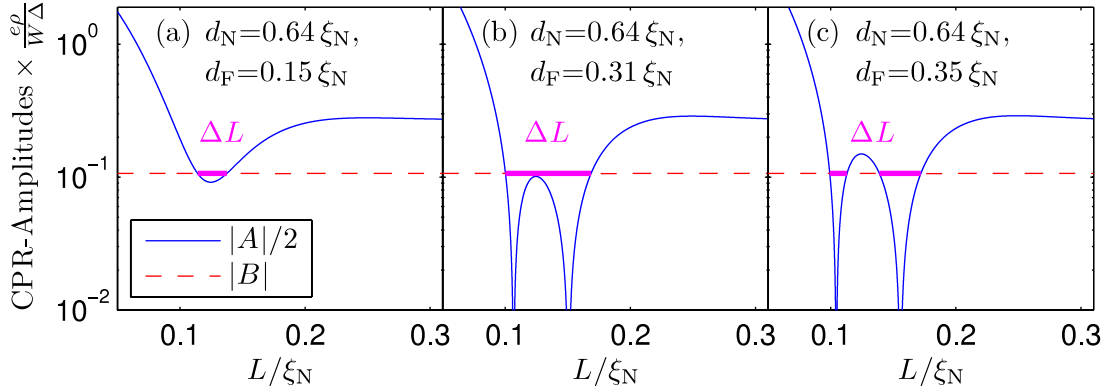


Figure 2. The functions $|A|/2$ and $|B|$, based on (28) and (29), as functions of L for $d_N = 0.64\xi_N$ and three characteristic values for d_F . The bold lines marked by ΔL correspond to values for L where the conditions (2) for φ junction realization are fulfilled.

is a result of [25]. It also has been calculated with the help of a solution for the non-linear Usadel equations because $\gamma_{BSF} = 0$ is assumed. Additionally the condition $\xi_F \ll L$ is required.

3.3. Composite NF current

We determine the current $I_{NF}(\phi)$ by combining the two non-linear solutions $\Phi_{F,dir}(x)$ and $\Phi_N(x)$ from (A.6) and (A.9) in the Appendix, respectively. The main idea is to decompose the ferromagnetic Green's function

$$\Phi_F(x, z) = \Phi_{F,dir}(x) + \Phi_{NF}(x, z) \quad (26)$$

into a function $\Phi_{F,dir}(x)$, which corresponds to currents only flowing in the F layer, and a function $\Phi_{NF}(x, z)$, which corresponds to currents flowing through the N layer into the F layer. The second function is obtained by linearizing the Usadel equations (3) in the F layer. Then we connect this to the N layer solution $\Phi_N(x)$ via the boundary conditions.

The superposition (26) of the solution $\Phi_{F,dir}$ for the non-linear Usadel equation with the solution Φ_{NF} for the linearized Usadel equation is valid because we distinguish in the F part between two cases: (i) at $x \approx \pm L/2$ near the boundaries to the S regions the Green's function $\Phi_{F,dir}$ is very dominant $|\Phi_{F,dir}| \gg |\Phi_{NF}|$ due to a transparent boundary between the S and the F part, that is $\gamma_{BSF} = 0$; (ii) at $x \approx 0$, that is away from the boundaries, the contribution of Φ_F decays exponentially. Therefore, the contribution from the N part is dominant $|\Phi_{NF}| \gg |\Phi_{F,dir}|$.

As a result (A.12) we obtain the current

$$\begin{aligned} \tilde{I}_{NF}(\phi) = & \frac{16 \cos(\phi/2) \xi_F}{\gamma_{BNF} \hbar \Delta \xi_N} e^{-\kappa L/2} \\ & \times \left[\sin \frac{\kappa L}{2} + \frac{\kappa L}{\sqrt{2}} e^{-\kappa L/2} \cos \left(\kappa L + \frac{\pi}{4} \right) \right] \\ & \times 2\pi T \sum_{\omega > 0} \Theta \Gamma(\phi) \sin \frac{\phi}{2}, \end{aligned} \quad (27)$$

with the definitions of $\Gamma(\phi)$ from (19), κ from (24) and Θ together with η from (25).

4. Discussion

In this section we estimate the geometrical parameters d_N , d_F and L , see figure 1, for which the considered Josephson

junction obeys the φ junction conditions (2). We use the analysing scheme of [18] and finally compare our results with the ones obtained in [18].

We split the sine series amplitudes

$$A = A_N + A_{F,dir} + A_{NF}, \quad (28)$$

$$B = B_N + B_{NF} \quad (29)$$

of the total current (16), scaled according to (17), into parts originating from the current of the N layer (18), the F layer (23) and the composite NF current (27). There is no amplitude $B_{F,dir}$ because we have a pure sinusoidal CPR (23) in the F layer.

In our calculations we chose the temperature $T = 0.1T_c$. We make this choice because far away from the critical temperature the CPR has larger deviations from the $\sin \phi$ form [22] which result in a larger second harmonic B . As S electrode material we chose Nb with $T_c = 9.2$ K because it is commonly used in superconducting circuits. Using these parameters, we checked that the amplitudes in front of the higher order sine terms are much smaller than A and B . Therefore it is justified to only take these two into account in the CPR (1) for our system.

In order to compare our system to that of [18] we first use the same parameters $d_N = 0.64\xi_N$, $\xi_F = 0.1\xi_N$, $H = 10T_c$, $\Delta = 1.76T_c$, $\rho_F = \rho_N = \rho$ and $\gamma_{BNF} = 1$ and analyse the amplitudes (28) and (29) as a function of L for different values of d_F . Figure 2 shows three typical examples: (a) $d_F = 0.15\xi_N$, (b) $d_F = 0.31\xi_N$ and (c) $d_F = 0.35\xi_N$. The first (a) and last (c) examples correspond to limiting cases where it is difficult to realize a φ junction because the intervals ΔL of L where conditions (2) hold are not large. These intervals ΔL are highlighted by bold lines. In between the two limiting values for d_F this line becomes longer. Figure 2(b) shows an optimum situation because there is a wide range for L which yields a φ junction configuration.

For the optimum value $d_F = 0.31\xi_N$ we calculate the magnitudes $\Upsilon_A = A_N W \Delta / (e\rho) = 0.534$ and $\Upsilon_B = B_N W \Delta / (e\rho) = -0.106$. Inserting these together with the amplitude $A_{F,dir}$ in front of $\sin \phi$ from (23) into (2) and neglecting the small NF contributions leads us to the condition

$$\left| \Upsilon_A + \frac{1}{\varepsilon} \Psi(L) \right| < 2 |\Upsilon_B|. \quad (30)$$

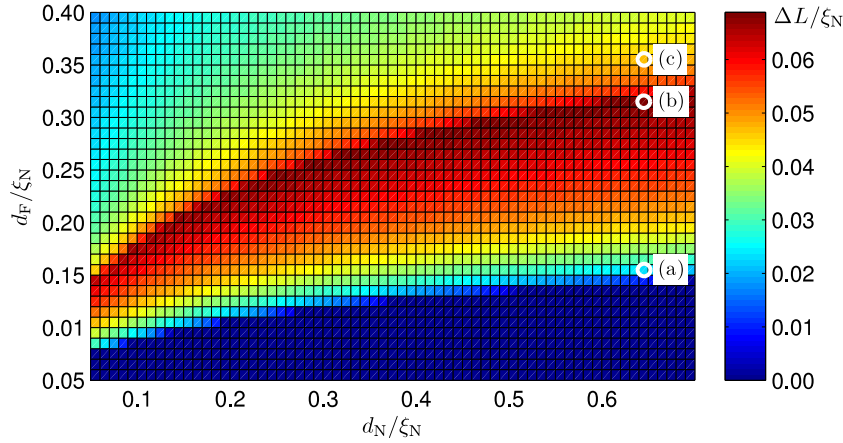


Figure 3. The range ΔL of possible values for the length L of the F layer for φ junction realization; it is more sensitive to changes of d_F than of d_N . Details for the parameters indicated by white circles are shown in figure 2(a)–(c), respectively.

Here, we use the constant $\varepsilon = \xi_F / (64\mathcal{F}\sqrt{hd_F})$ with $d_F = 0.31\xi_N$, $\mathcal{F} = 0.0691$ and

$$\Psi(L) = \exp(-2\kappa L) \sin(2\kappa L + \pi/4). \quad (31)$$

From (30) we find the minimum value $0.10\xi_N$ and the maximum value $0.17\xi_N$ for L .

To analyse the situation for values of d_N other than $0.64\xi_N$ we plot in figure 3 the length ΔL of the bold line shown in figure 2 as a function of d_N and d_F . In case this bold line gets split, as shown in figure 2(c), we calculate ΔL by summing up the fragments. When ΔL becomes larger, the realization of a φ junction becomes easier because more lengths L of the F layer are suitable. For small values of d_F no φ junction realization is possible. This can be explained with the help of figure 2(a) by imagining that the minimum of the $|A|/2$ curve exceeds the dashed line $|B|$ for small values of d_F . The probability of finding a φ junction experimentally is less sensitive to changes of d_N than of d_F .

For summarizing our suggestion for the geometrical configuration of a φ junction we use the value $\xi_N = 100$ nm for Cu as the N layer, and a strongly diluted ferromagnet such as FePd or the CuNi alloy with $\xi_N = 10$ nm and $H = 10T_c$ as the F metal. Our set of parameters then becomes $d_N \gtrsim 50$ nm, 15 nm $\lesssim d_F \lesssim 35$ nm and 10 nm $\lesssim L \lesssim 17$ nm, which we compare to the values $d_N \gtrsim 50$ nm, 19 nm $\lesssim d_F \lesssim 48$ nm and 7 nm $\lesssim L \lesssim 22$ nm.⁵

Since we use the same N layer configuration, the value for d_N is the same, but the suggested regime for d_F differs. A change in this direction was expected because we only need a thin F layer since the transparency of our interfaces already amplifies our SFS current contribution. The possible range for the length L of the F part is smaller in our case but the whole junction configuration is still experimentally feasible.

5. Conclusion

We have shown that the considered Josephson junction with a ferromagnetic weak link located on a thin normal metal film

is a good candidate for φ junction realization. By choosing transparent SF interfaces we obtained slightly different system sizes for φ junction existence compared with a junction with weakly transparent interfaces.

The current was split into a contribution through the N layer, the F layer and a composite term which described the current flowing through the N and F parts of the junction simultaneously. We performed our calculations in the ‘dirty’ limit, that is the currents are obtained from solutions for the non-linear Usadel equations.

Since our case of a large interface transparency corresponds better to the experimental situation [23, 24, 19] than weakly transparent interfaces (see footnote 5) it is important to note that a smaller thickness and length for the F layer have to be chosen than predicted (see footnote 5). We are looking forward to experiments realizing this φ junction and its applications in classical and quantum devices.

Acknowledgments

We thank S V Bakurskiy for fruitful and stimulating discussions. DMH thanks Professor W P Schleich and K Vogel for giving him the possibility to work at the M V Lomonosov Moscow State University. Financial support by the German Science Foundation (DFG) in the framework of the SFB/TRR-21, the Russian Foundation for Basic Research (RFBR grants Nos 11-02-12065-ofi-m, 13-02-01452-a) and the Ministry of Education and Science of the Russian Federation (grant 8641) is gratefully acknowledged.

Appendix. NF current derivation

In this appendix we derive the current (27) which flows through the N and F part of the junction, sketched in figure 1, simultaneously. We first linearize the Usadel equations (3) and then combine the solution with the Green’s functions from [18, 25].

For the linearization of (3) we assume the superconducting correlation coming from the N part into the F part as rather small. Then, the Green’s function $\Phi_{NF}(x, z)$ can also

⁵ Estimates for the thickness d_F of an RTO φ junction with weakly transparent SF interfaces are taken from [18] and divided by a missing factor π .

be assumed to be small. Using $G_{\text{NF}} = \text{sign}(\omega)$ we obtain the linearized Usadel equation [21]

$$\xi_{\text{F}}^2 \left(\frac{\partial^2}{\partial x^2} + \frac{\partial^2}{\partial z^2} \right) \Phi_{\text{NF}} = \tilde{\Omega} \Phi_{\text{NF}}, \quad (\text{A.1})$$

with the definitions

$$\tilde{\Omega} = |\Omega| + i \text{sign}(\Omega)h, \quad \Omega = \frac{\omega}{\pi T_{\text{c}}}, \quad h = \frac{H}{\pi T_{\text{c}}}. \quad (\text{A.2})$$

Its solution in the form of a series

$$\begin{aligned} \Phi_{\text{NF}}(x, z) \\ = \sum_{n=1}^{\infty} b_n \sin\left(\frac{2\pi}{L}nx\right) \cosh[\kappa_n(z - d_{\text{N}} - d_{\text{F}})], \end{aligned} \quad (\text{A.3})$$

with

$$\kappa_n^2 = \left(\frac{2\pi n}{L}\right)^2 + \frac{\tilde{\Omega}}{\xi_{\text{F}}^2} \quad (\text{A.4})$$

and a Fourier coefficient b_n , already obeys the boundary condition (8) at the upper border ($z = d_{\text{N}} + d_{\text{F}}$).

The boundary conditions at the left and right end of the F part at $x = \pm L/2$ are also already fulfilled. They follow from (10) with $\gamma_{\text{BSF}} = 0$. Using here the definition (26) for Φ_{F} leads us to the condition

$$\Phi_{\text{F,dir}}(\pm L/2) + \Phi_{\text{NF}} = \frac{\tilde{\Omega}}{\Omega} \Phi_{\text{S}}(\pm L/2). \quad (\text{A.5})$$

This equation is already fulfilled by the solution

$$\Phi_{\text{F,dir}}(x) = \frac{\tilde{\Omega}}{G_{\text{F,dir}}} \left(e^{-i\phi/2} \sin \alpha^- + e^{+i\phi/2} \sin \alpha^+ \right) \quad (\text{A.6})$$

with

$$\alpha^{\pm} = 4 \arctan \left[\Theta \exp \left(\pm \sqrt{\tilde{\Omega}} \frac{x \mp L/2}{\xi_{\text{F}}} \right) \right], \quad (\text{A.7})$$

$$\Theta = \frac{\Delta}{\eta + |\omega| + \sqrt{2\eta(\eta + |\omega|)}}, \quad (\text{A.8})$$

from [25] alone. Therefore, the NF Green's function (A.3) only has to obey the conditions $\Phi_{\text{NF}} = 0$ at $x = \pm L/2$. Note that we do not need the expression for $G_{\text{F,dir}}$ to finally calculate the current.

In order to obtain the Fourier coefficient b_n which fixes the solution Φ_{NF} from (A.3) we use the boundary condition (11) where we neglect the term Φ_{NF} assuming $|\Phi_{\text{NF}}| \ll |\Phi_{\text{N}}|$. Now, we replace the Green's function G_{F} by $G_{\text{NF}} = \text{sign}(\omega)$ and insert

$$\begin{aligned} \Phi_{\text{N}}(x) = r\Delta \cos \frac{\phi}{2} + 2i\mu(\phi)\Gamma(\phi) \sin\left(\frac{\phi}{2}\right) \frac{x}{\xi_{\text{N}}}, \\ G_{\text{N}} = \frac{\Omega}{\mu(\phi)}, \end{aligned} \quad (\text{A.9})$$

from [18], where we use the definitions (19), (21) and (22) for $\Gamma(\phi)$, r and $\mu(\phi)$, respectively. By neglecting the real part of Φ_{N} we obtain the Fourier coefficient

$$b_n = \frac{2i \tilde{\Omega} L (-1)^n \Gamma(\phi) \sin(\phi/2)}{\kappa_n \sinh(\kappa_n d_{\text{F}}) \xi_{\text{F}} \gamma_{\text{BNF}} \pi n \xi_{\text{N}}}. \quad (\text{A.10})$$

Our last step is to calculate the current I_{NF} . Therefore, we insert the Green's function (26), which contains the Green's functions from (A.3) and (A.6), into the definition (15) for the F layer current. Due to the condition $x = 0$ this reduces to a sum $I_{\text{F}}(\phi) = I_{\text{NF}}(\phi) + I_{\text{F,dir}}(\phi)$, where the NF current is defined by

$$\begin{aligned} I_{\text{NF}}(\phi) = i \frac{\pi T W}{2e \rho_{\text{F}}} \sum_{\omega=-\infty}^{\infty} \int_{d_{\text{N}}}^{d_{\text{N}}+d_{\text{F}}} dz \frac{G_{\text{NF}} G_{\text{F,dir}}}{\tilde{\omega}^2} \\ \times \left[\Phi_{\text{F,dir}}(\omega) \frac{\partial}{\partial x} \Phi_{\text{NF}}^*(-\omega) \right. \\ \left. - \Phi_{\text{F,dir}}^*(-\omega) \frac{\partial}{\partial x} \Phi_{\text{NF}}(\omega) \right]_{x=0} \end{aligned} \quad (\text{A.11})$$

and $I_{\text{F,dir}}(\phi)$ is the current flowing only through the F layer [25] summarized in (23).

We insert the Green's functions Φ_{NF} and $\Phi_{\text{F,dir}}$ from (A.3) and (A.6) into (A.11). Then, by finally using the approximation $\tilde{\Omega} \approx ih$, which holds for the condition $\pi T_{\text{c}} \ll H$, we obtain the scaled current

$$\begin{aligned} \tilde{I}_{\text{NF}}(\phi) = \frac{16 \cos(\phi/2) \xi_{\text{F}} e^{-\kappa L/2}}{\gamma_{\text{BNF}} h \Delta \xi_{\text{N}}} \\ \times \left[\sin \frac{\kappa L}{2} + \frac{\kappa L}{\sqrt{2}} e^{-\kappa L/2} \cos\left(\kappa L + \frac{\pi}{4}\right) \right] \\ \times 2\pi T \sum_{\omega>0} \Theta \Gamma(\phi) \sin \frac{\phi}{2}. \end{aligned} \quad (\text{A.12})$$

References

- [1] Mints R G 1998 *Phys. Rev. B* **57** R3221–4
- [2] Buzdin A and Koshelev A E 2003 *Phys. Rev. B* **67** 220504
- [3] Goldobin E, Koelle D, Kleiner R and Buzdin A 2007 *Phys. Rev. B* **76** 224523
- [4] Bulaevskii L N, Kuzii V V and Sobyenin A A 1977 *JETP Lett.* **25** 290
- [5] Ustinov A V and Kaplunenko V K 2003 *J. Appl. Phys.* **94** 5405–7
- [6] Ortlepp T, Ariando, Mielke O, Verwijs C J M, Foo K F K, Rogalla H, Uhlmann F H and Hilgenkamp H 2006 *Science* **312** 1495–7
- [7] Feofanov A K, Oboznov V A, Bol'ginov V V, Lisenfeld J, Poletto S, Ryazanov V V, Rossolenko A N, Khabipov M, Balashov D, Zorin A B, Dmitriev P N, Koshelets V P and Ustinov A V 2010 *Nature Phys.* **6** 593–7
- [8] Il'ichev E, Zakosarenko V, IJsselsteijn R P J, Hoenig H E, Meyer H G, Fistul M V and Müller P 1999 *Phys. Rev. B* **59** 11502–5
- [9] Cleuziou J P, Wernsdorfer W, Bouchiat V, Ondarçuhu T and Monthieux M 2006 *Nature Nanotechnol.* **1** 53–9
- [10] Gumann A and Schopohl N 2009 *Phys. Rev. B* **79** 144505
- [11] Pugach N G, Goldobin E, Kleiner R and Koelle D 2010 *Phys. Rev. B* **81** 104513
- [12] Goldobin E, Koelle D, Kleiner R and Mints R G 2011 *Phys. Rev. Lett.* **107** 227001
- [13] Lipman A, Mints R G, Kleiner R, Koelle D and Goldobin E 2012 arXiv:1208.4057
- [14] Alidoust M and Linder J 2013 *Phys. Rev. B* **87** 060503
- [15] Sickinger H, Lipman A, Weides M, Mints R G, Kohlstedt H, Koelle D, Kleiner R and Goldobin E 2012 *Phys. Rev. Lett.* **109** 107002

- [16] Smilde H J H, Ariando, Blank D H A, Gerritsma G J, Hilgenkamp H and Rogalla H 2002 *Phys. Rev. Lett.* **88** 057004
- [17] Weides M, Kemmler M, Kohlstedt H, Waser R, Koelle D, Kleiner R and Goldobin E 2006 *Phys. Rev. Lett.* **97** 247001
- [18] Bakurskiy S V, Klenov N V, Karminskaya T Y, Kupriyanov M Y and Golubov A A 2012 *Supercond. Sci. Technol.* **26** 015005
- [19] Golikova T E, Hübler F, Beckmann D, Batov I E, Karminskaya T Y, Kupriyanov M Y, Golubov A A and Ryazanov V V 2012 *Phys. Rev. B* **86** 064416
- [20] Golubov A A, Kupriyanov M Y and Il'ichev E 2004 *Rev. Mod. Phys.* **76** 411–69
- [21] Buzdin A I 2005 *Rev. Mod. Phys.* **77** 935–77
- [22] Likharev K K 1979 *Rev. Mod. Phys.* **51** 101–59
- [23] Oboznov V A, Bol'ginov V V, Feofanov A K, Ryazanov V V and Buzdin A I 2006 *Phys. Rev. Lett.* **96** 197003
- [24] Bannykh A A, Pfeiffer J, Stolyarov V S, Batov I E, Ryazanov V V and Weides M 2009 *Phys. Rev. B* **79** 054501
- [25] Buzdin A I and Kupriyanov M Y 1991 *JETP Lett.* **53** 321–6
- [26] Usadel K D 1970 *Phys. Rev. Lett.* **25** 507–9
- [27] Kupriyanov M Y and Lukichev V F 1988 *Zh. Eksp. Teor. Fiz.* **94** 139–49
- [28] Koshina E A and Krivoruchko V N 2000 *Low Temp. Phys.* **26** 115–20